Journal of Applied Electrochemistry **31**: 79–83, 2001.

An investigation of some Schiff bases as corrosion inhibitors for austenitic chromium–nickel steel in H_2SO_4

S. BİLGİÇ* and N. ÇALISKAN
Department of Physical Chemistry, Ankara University, Beşevler, Ankara, Turkey
*(*author for correspondence, fax: +90 312 223 23 95, e-mail: bilgic@science.ankara.edu.tr)*

Received 8 December 1999; accepted in revised form 20 July 2000

Key words: corrosion, inhibitor, Schiff bases, steel

Abstract

The corrosion inhibition of austenitic chromium–nickel steel by two Schiff bases, *N*-(1-toluidine)salicylaldimine and *N*-(2-hydroxyphenyl)salicylaldimine, was investigated in sulphuric acid medium. The effect of concentration and temperature on inhibition properties was determined. It was found that when the concentrations of inhibitor were increased the inhibition efficiencies (η) and surface coverage (θ) increased. Some thermodynamic parameters such as free energy of adsorption, ΔG°_{ads}, and enthalpy, ΔH, were determined for the Schiff bases. Experimental results agree with the Temkin isotherm for *N*-(1-toluidine)salicylaldimine, but the Langmuir isotherm is more appropriate for *N*-(2-hydroxyphenyl)salicylaldimine.

1. Introduction

The use of inhibitors is one of the most practical methods for protection against corrosion in acidic media [1]. As acidic media HCl and H_2SO_4 are generally used in the treatment of steel and ferrous alloys. Most of the well known acid inhibitors are organic compounds containing nitrogen, sulphur and oxygen atoms [2–8]. The influence of heterocyclic compounds and other organics containing nitrogen, such as amines and amino acids, on the corrosion of steel in acidic solutions has been investigated by several workers [9–15].

Several Schiff bases have recently been investigated as corrosion inhibitors for various metals and alloys in acidic media [16–20]. The aim of this study is to investigate the inhibitive properties of two Schiff bases, *N*-(1-toluidine)salicylaldimine, and *N*-(2-hydroxyphenyl)salicylaldimine on the corrosion of austenitic chromium–nickel steel in sulphuric acid. The chemical structures of the two Schiff bases are given in Figure 1.

2. Experimental details

Electrochemical experiments were carried out in a Pyrex cell with three compartments. An austenitic chromium–nickel steel with the composition shown in Table 1 was used in the study. This steel electrode, 5 mm in diameter, was embedded in a polyester resin, mechanically polished with 1200 grit, emery paper, washed in bidistilled water and then placed in the test solution. All solutions were deaerated with nitrogen for 30 min in the cell prior to each experiment. Oxygen was removed from the nitrogen used by passing through pyrogallol, vanadium chloride and hydrochloric acid. During each experiment, solutions were mixed with a magnetic stirrer. Inhibitor concentrations were chosen as 1×10^{-3}, 3×10^{-3}, 5×10^{-3}, 1×10^{-2} and 2×10^{-2} M. A saturated calomel electrode (SCE) was used as reference and a platinum plate as counter electrode. All potentials were referred to SCE. The cell was water-jacketed and was connected to a constant temperature circulator. Experiments were carried out at 298, 308, 318, 328 and 338 K.

Data were obtained using a combined system containing a Wenking LB 75 L laboratory model potentiostat, a Wenking model VS G 72 voltage scan generator and a type 3077 Yokogawa recorder. The potential sweep rate was 2.5 mV s^{-1}. The potential was scanned in the negative direction from E_{cor}, and subsequently in the positive direction.

3. Results and discussion

Figure 2 gives the anodic and cathodic polarization curves at 298 K in 0.5 M H_2SO_4 in the absence and presence of various concentrations of *N*-(1-toluidine)salicylaldimine. Figure 3 represents the anodic and cathodic polarization curves at the same temperature in 0.5 M H_2SO_4 for *N*-(2-hydroxyphenyl)salicylaldimine. Corrosion current densities, percentage inhibition efficiencies and degrees of surface coverage can be seen in Tables 2 and 3 for *N*-(1-toluidine)salicylaldimine and *N*-(2-hydroxyphenyl)salicylaldimine, respectively.

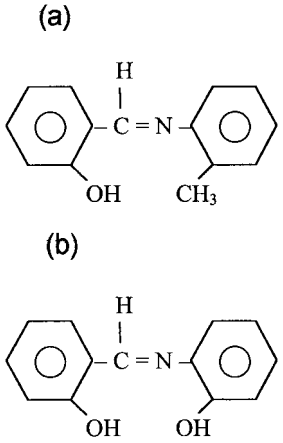

Fig. 1. Chemical structures of Schiff bases studied: (a) *N*-(1-toluidine)salicylaldimine; (b) *N*-(2-hydroxyphenyl)salicylaldimine.

The percentage inhibition efficiency, η, and the surface coverage, θ, were calculated from the following equations:

$$\eta = \left(\frac{i_0 - i_1}{i_0}\right) \times 100 \tag{1a}$$

$$\theta = \frac{i_0 - i_1}{i_0} \tag{1b}$$

where i_0 and i_1 are the corrosion current densities without and with inhibitor. With an increase in the concentration of the Schiff base, both anodic and cathodic currents were inhibited more effectively, but the reduction in the anodic currents was greater than in those of the cathodic currents. Corrosion potentials also shifted in the positive direction.

As the electrochemical processes on the metal surface is likely to be closely related to the adsorption of the inhibitor, [21–23] and the adsorption is known to depend on the chemical structure of the inhibitor [2–10], we decided to study the adsorption of the Schiff bases on the steel surface.

The adsorption of inhibitor molecules from an aqueous solution can be regarded as a quasisubstitution process between the organic compound in the aqueous phase org(aq) and water molecules at the electrode surface, $H_2O(s)$.

$$\mathrm{Org(aq)} + x\mathrm{H_2O(s)} \rightleftharpoons \mathrm{Org(s)} + x\mathrm{H_2O} \tag{2}$$

where x, the size ratio, is the number of water molecules displaced by one molecule of organic inhibitor.

Adsorption isotherms are very important in determining the mechanism of organo-electrochemical reactions. The most frequently used isotherms are

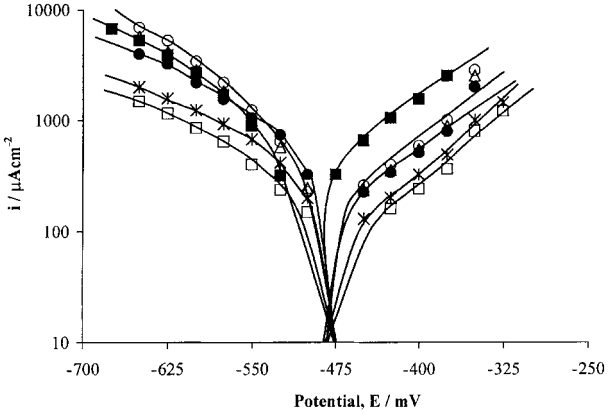

Fig. 2. Anodic and cathodic polarization curves at 298 K in 0.5 M H_2SO_4 in various concentrations of *N*-(1-toluidine)salicylaldimine. Key: (■) 0.5 M H_2SO_4, (○) 0.5 M H_2SO_4 + 1×10^{-3} M, (△) 0.5 M + 3×10^{-3} M, (●) 0.5 M H_2SO_4 + 5×10^{-3} M, (✳) 0.5 M H_2SO_4 + 1×10^{-2} M, (□) 0.5 M H_2SO_4 + 2×10^{-2} M.

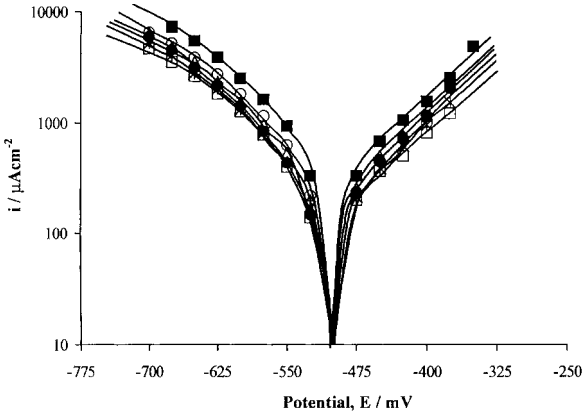

Fig. 3. Anodic and cathodic polarization curves at 298 K in 0.5 M H_2SO_4 in various concentrations of *N*-(2-hydroxyphenyl)salicylaldimine. Key: (■) 0.5 M H_2SO_4, (○) 0.5 M H_2SO_4 + 1×10^{-3} M, (△) 0.5 M + 3×10^{-3} M, (●) 0.5 M H_2SO_4 + 5×10^{-3} M, (✳) 0.5 M H_2SO_4 + 1×10^{-2} M, (□) 0.5 M H_2SO_4 + 2×10^{-2} M.

Langmuir, Frumkin, Hill de Boer, Parsons, Temkin, Flory–Huggins and Dhar–Flory–Huggins and Bockris–Swinkels [24–29]. All these isotherms are of the general form:

$$f(\theta, x)\exp(-2a\theta) = KC \tag{3}$$

where $f(\theta, x)$ is the configurational factor which depends upon the physical model and the assumptions underlying the derivation of the isotherm [10], θ is the degree of surface coverage, C is the inhibitor concentration in the electrolyte, x is the size ratio, a is the molecular interaction parameter, and K is the equilibrium constant of the adsorption process. For *N*-(1-toluidine)salicyl-

Table 1. Chemical composition (wt %) of steel used as electrode

C	Si	Mn	P	S	Cr	Mo	Ni	Al	Co	Cu	Fe
0.0425	0.0421	2.13	0.0133	0.113	0.358	0.563	8.64	0.0334	0.0501	0.358	balance

Table 2. Corrosion current densities, i_{cor}, inhibition efficiencies, (η), and surface coverage degrees, θ, in various concentrations of *N*-(1-toluidine)salicylaldimine at different temperatures

Temperature /K	Concentration /M	Corrosion rate i_{cor} /μA cm^{-2}	Inhibition efficiency /η%	Surface coverage /θ
298	H_2SO_4	400	–	–
	1×10^{-3}	250	37	0.37
	3×10^{-3}	235	41	0.41
	5×10^{-3}	220	45	0.45
	1×10^{-2}	170	57	0.57
	2×10^{-2}	130	67	0.67
308	H_2SO_4	1000	–	–
	1×10^{-3}	600	40	0.40
	3×10^{-3}	450	55	0.55
	5×10^{-3}	350	65	0.65
	1×10^{-2}	230	77	0.77
	2×10^{-2}	205	79	0.79
318	H_2SO_4	4200	–	–
	1×10^{-3}	1600	61	0.61
	3×10^{-3}	1100	73	0.73
	5×10^{-3}	900	78	0.78
	1×10^{-2}	540	87	0.87
	2×10^{-2}	260	93	0.93
328	H_2SO_4	5500	–	–
	1×10^{-3}	2000	63	0.63
	3×10^{-3}	1500	72	0.72
	5×10^{-3}	1000	81	0.81
	1×10^{-2}	700	87	0.87
	2×10^{-2}	400	92	0.92
338	H_2SO_4	8400	–	–
	1×10^{-3}	3000	67	0.67
	3×10^{-3}	2400	71	0.71
	5×10^{-3}	1400	83	0.83
	1×10^{-2}	900	89	0.89
	2×10^{-2}	600	93	0.93

Table 3. Corrosion current densities, i_{cor}, inhibiton efficiencies, (η) and surface coverage degrees, θ, in various concentrations of *N*-(2-hydroxyphenyl)salicylaldimine at different temperatures

Temperature /K	Concentration /M	Corrosion rate i_{cor} /μA cm^{-2}	Inhibition efficiency /η%	Surface coverage /θ
298	H_2SO_4	400	–	–
	1×10^{-3}	285	28	0.28
	3×10^{-3}	260	35	0.35
	5×10^{-3}	250	37	0.37
	1×10^{-2}	200	50	0.50
	2×10^{-2}	180	55	0.55
308	H_2SO_4	1000	–	–
	1×10^{-3}	700	30	0.30
	3×10^{-3}	560	44	0.44
	5×10^{-3}	480	52	0.52
	1×10^{-2}	400	60	0.60
	2×10^{-2}	235	76	0.76
318	H_2SO_4	4200	–	–
	1×10^{-3}	2600	38	0.38
	3×10^{-3}	1600	61	0.61
	5×10^{-3}	1100	73	0.73
	1×10^{-2}	440	89	0.89
	2×10^{-2}	300	92	0.92
328	H_2SO_4	5500	–	–
	1×10^{-3}	3100	43	0.43
	3×10^{-3}	2100	61	0.61
	5×10^{-3}	1800	67	0.67
	1×10^{-2}	530	90	0.90
	2×10^{-2}	420	92	0.92
338	H_2SO_4	8400	–	–
	1×10^{-3}	4300	48	0.48
	3×10^{-3}	3100	63	0.63
	5×10^{-3}	2400	71	0.71
	1×10^{-2}	700	92	0.92
	2×10^{-2}	520	93	0.93

aldimine, it was found that the Temkin adsorption isotherm fits best to the experimental results over the temperature range studied. Starting with the Temkin isotherm.

$$\exp(-2a\theta) = KC \tag{4}$$

and rearranging gives

$$\theta = -\frac{1}{2a}\ln K - \frac{1}{2a}\ln C \tag{4'}$$

This equation shows that a plot of θ against ln C must be linear provided that the assumptions of the Temkin isotherm are valid.

Figure 4 shows the experimental data obtained at various temperatures. These curves can be regarded as straight lines and therefore the adsorption process follows the Temkin isotherm.

However, for *N*-(2-hydroxyphenyl)salicylaldimine adsorption, data agree with the Langmuir adsorption isotherm, which is valid when $a = 0$ and $x = 1$. Starting with the conventional form of the Langmuir isotherm, that is,

$$\frac{\theta}{1-\theta} = KC \tag{5}$$

and rearranging gives

$$\frac{C}{\theta} = \frac{1}{K} + C \tag{5'}$$

A graph of C/θ against C leads to values K.

Figure 5 shows the graphical form of the data and the points fit the Langmuir isotherm well.

The difference in the adsorption behaviour of the two Schiff bases can be tentatively attributed to the structures of these molecules. Supposing these molecules are attached to the solid surface through coordination bonds formed by the electron-donating N or O atoms, *N*-(1-toluidine)salicylaldimine might be attached to the surface with one site leaving the other donor atom free to form intermolecular hydrogen bonds with the molecules of the second layer. However, the Schiff base *N*-(2-hydroxyphenyl)salicylaldimine has two closely-spaced OH groups that may well be used in forming an intramolecular hydrogen bond, in which case only the C=N group would be available to link the molecule

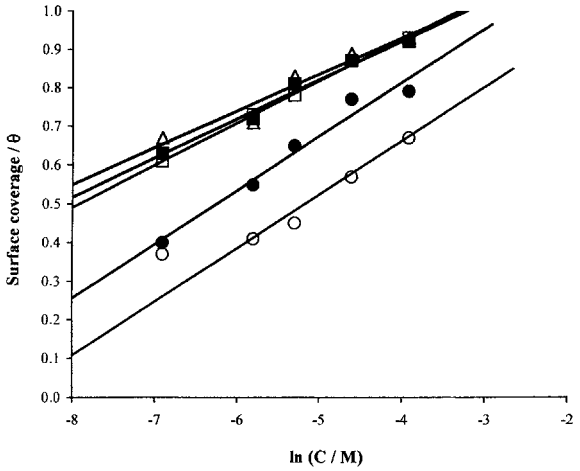

Fig. 4. Experimental results over 298–338 K according to the Temkin isotherm for *N*-(1-toluidine)salicylaldimine. Key: (○) 298, (●) 308, (□) 318, (■) 328 and (△) 338 K.

to the surface. In this circumstance multilayer adsorption would be unlikely and obediance to the Langmuir isotherm becomes reasonable.

The free energies of adsorption, ΔG°_{ads}, were calculated from the equilibrium constant of adsorption using the following equation:

$$K = \frac{1}{55.5}\exp\left(-\frac{\Delta G^{\circ}_{ads}}{RT}\right) \quad (6)$$

The variation of $\Delta G^{\circ}_{ads}/T$ with $1/T$ was obtained using the Gibbs–Helmholtz equation and is shown in Figure 6 for *N*-(1-toluidine)salicylaldimine. The similar variation of $\Delta G^{\circ}_{ads}/T$ with $1/T$ is depicted in Figure 7 for the other Schiff base, *N*-(2-hydroxyphenyl)salicylaldimine. It can be seen that $\Delta G^{\circ}_{ads}/T$ decreases with $1/T$ in approximately linear fashion. These results indicate the spontaneous adsorption of both inhibitor molecules. However, the slopes of the graphs are different.

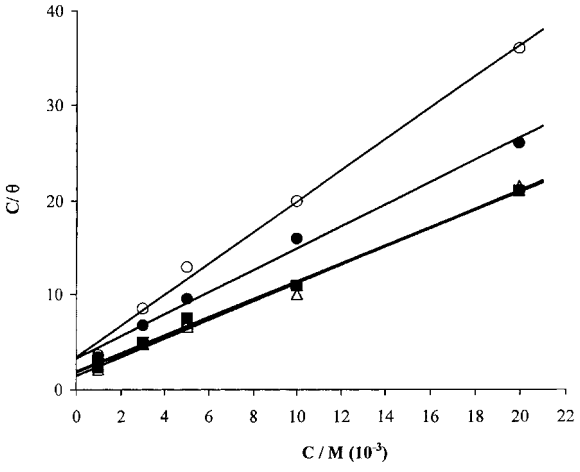

Fig. 5. Experimental results over 298–338 K according to the Langmuir isotherm for *N*-(2-hydroxyphenyl)salicylaldimine. Key: (○) 298, (●) 308, (□) 318, (■) 328 and (△) 338 K.

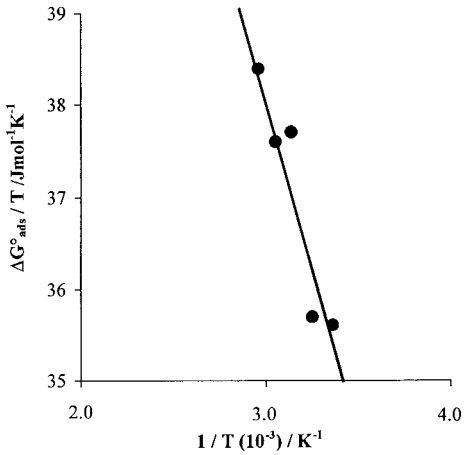

Fig. 6. Variation of $\Delta G^{\circ}_{ads}/T$ with $1/T$ for *N*-(1-toluidine)salicylaldimine.

Chemisorption involves charge sharing or charge transfer from the inhibitor molecules to the surface to form a coordination bond. In fact, electron transfer is typical for transition metals having vacant, low-energy electron orbitals. Electron transfer can be expected with compounds having relatively loosely bound electrons [30]. The number of π electrons in the system is then likely to be the determining factor in the adsorption process. This has been proved by several investigators [31–33].

Iron is well known for its coordination affinity to nitrogen and oxygen bearing ligands [34–36]. Therefore adsorption on steel may also be attributed to coordination through phenolic OH and C=N groups. Efficient adsorption of the inhibitor molecules may be either due to π-electrons of the aromatic system or electronegative donor atoms, N and O. The inhibition efficiencies of both Schiff bases show almost the same pattern. This is expected, taking into account the similar structures of the two molecules.

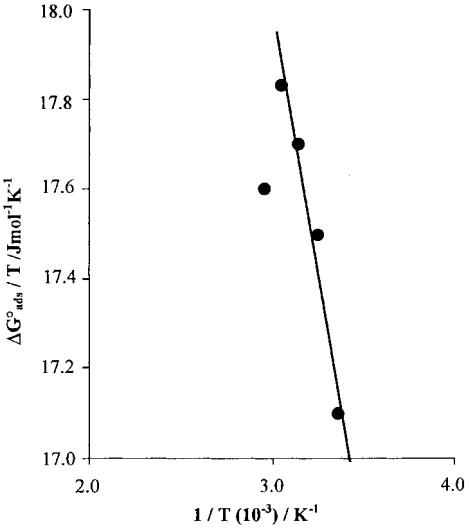

Fig. 7. Variation of $\Delta G^{\circ}_{ads}/T$ with $1/T$ for *N*-(2-hydroxyphenyl)salicylaldimine.

6. Conclusions

The following conclusions can be drawn from this study:

(i) The adsorption enthalpies, ΔH, from the Gibbs–Helmholtz equation were found to be -7549 J mol^{-1} for *N*-(1-toluidine)salicylaldimine, and -2303 J mol^{-1} for *N*-(2-hydroxyphenyl)salicylaldimine. That the first Schiff base is adsorbed more strongly on the steel surface is confirmed by these ΔH values and also by the relevant Temkin isotherms.

(ii) Both Schiff bases investigated act anodically and cathodically as inhibitors, but their efficiencies appear to be better when they are used in anodic measurements. This point was elucidated by inspection of the Tafel slopes.

(iii) That the adsorption of *N*-(1-toluidine)salicylaldimine obeys the Temkin (multilayer) isotherm whereas the adsorption of *N*-(2-hydroxyphenyl)salicylaldimine follows the Langmuir (monolayer) isotherm may be explained on the basis of the fact that the first Schiff base is more prone to intermolecular hydrogen bonding and the second contains two closely-spaced OH groups, making the molecule highly likely to form intramolecular bonds.

Acknowledgement

The authors wish to thank H. Yılmaz of the Ankara University. Inorganic Chemistry Department for his valuable contributions on the evaluation of the data.

References

1. G. Trabanelli, *Corrosion* **47** (1991) 410.
2. S.N. Raicheva, B.V. Aleksiev and E.I. Sokolova, *Corros. Sci.* **34** (1993) 343.
3. V. Hluchan, B.L. Wheeler and N. Hackerman, *Werkst. Korros.* **39** (1998) 512.
4. A. Frignani, M. Tassinari, Proceedings of the 7th European Symposium on 'Corrosion Inhibitors', N.S. Sez V. Supp. 9, Ann. Univ. Ferrara, Italy (1990), p. 895.
5. D.P. Schweinsberg and V. Ashworth, *Corros. Sci.* **28** (1988) 539.
6. A. Frignani, C. Monticelli, G. Brunoro, M. Zucchi and I. Hashi Omar, *Br. Corros. J.* **22** (1987) 103.
7. M. Bouayed, H. Rabaā, A. Srhiri, J.-Y. Saillard, A. Ben Bachir and A. Le Beuze, *Corros. Sci.* **41** (1999) 501.
8. X.L. Cheng, H.Y. Ma, S.H. Chen, R.Yu, X. Chen and Z.M. Yao, *Corros. Sci.* **41** (1999) 321.
9. G. Moretti, G. Quartarone, A. Tassan and A. Zingales, *Werkst. Korros.* **45** (1994) 641.
10. B.G. Ateya, B.E. El-Anadouli and F.M. El-Nizamy, *Corros. Sci.* **24** (1984) 509.
11. S. Kertit, B. Hammouti, M. Taleb and M. Brighli, *Bull. Electrochem.* **13** (1997) 241.
12. F. Zucchi and G. Trabanelli, Proceedings of the 7th European Symposium on 'Corrosion Inhibitors', (7 SEIC) Ann. Univ. Ferrara, Sez. V, Italy (1990) p. 339.
13. A. Srhiri, M. Etman and F. Dabosi, *Electrochim. Acta* **41** (1996) 429.
14. F. Bentiss, M. Lagrenee, M. Traisnel and J.C. Hornez, *Corros. Sci.* **41** (1999) 789.
15. J.M. Sykes, *Br. Cor. J.* **25** (1990) 175.
16. M.N. Desai, M.B. Desai, C.B. Shah and S.M. Desai, *Corros. Sci.* **26** (1986) 827.
17. M.N. Desai, P.O. Chauhan and N. Shah, Proceedings of 7th European Symposium on 'Corrosion Inhibitors', Sez V. Ann. Univ. Ferrara, Italy (1990), p. 1199.
18. H. Shokry, M. Yuasa, I. Sekine, R.M. Issa, H.Y. El-Baradie and G.K. Gomma, *Corros. Sci.* **40** (1999) 2173.
19. S. Li, S. Chen, S. Lei, H. Ma, R. Yu and D. Liu, *Corros. Sci.* **41** (1999) 1273.
20. S.L. Li, Y.G. Wang, S.H. Chen, R. Yu, S.B. Lei, H.Y. Ma and De X Liu, *Corros. Sci.* **41** (1999) 1769.
21. N. Hackerman, J.D. Sudbury, *J. Electrochem. Soc.* **94** (1950) 4.
22. N. Hackerman, *Corrosion* **18** (1962) 332 t.
23. J.O'M. Bockris, A.K.N. Reddy, 'Modern Electrochemistry 2' (Plenum/Rosetta edition, New York, 1977), p. 792.
24. A.N. Frumkin, *Z. Phys. Chem.* **116** (1925) 466.
25. O. Ikeda, H. Jimbo and H. Tamura, *J. Electroanal. Chem.* **137** (1982) 127.
26. H. de Boer, 'The Dynamical Character of Adsorption', 2nd edn (Claredon Press, Oxford, 1968).
27. R. Parsons, *J. Electroanal. Chem.* **7** (1964) 136.
28. H.P. Dhar, B.E. Conway and K.M. Joshi, *Electrochim. Acta* **18** (1973) 789.
29. J.O'M. Bockris, D.A.J. Swinkels, *J. Electrochem. Soc.* **111** (1964) 736.
30. G. Trabanelli, *in* F. Mansfield (Ed), 'Corrosion Mechanisms' (Marcel Dekker, New York, 1987), p. 119.
31. I.L. Rosenfeld, 'Corrosion Inhibitors' (McGraw-Hill, New York, 1981), p. 98.
32. G. Okamoto, M. Nagayama, J. Kato and T. Baba, *Corros. Sci.* **2** (1962) 21.
33. T. Kristof and T. Salamon, *Werkst. Korros.* **41** (1990) 519.
34. M.K. Donal Jr, *Chem. Rev.* **90** (1990) 585.
35. B.S. Synder, G.S. Patterson, A.J. Abrahamson and R.H. Holm, *J. Am. Chem. Soc.* **111** (1989) 5214.
36. W.L. Jolly, 'Modern Inorganic Chemistry', 2nd edn (McGraw-Hill, New York, 1976), p. 408.